A model for the delamination kinetics of $La_{0.8}Sr_{0.2}MnO_3$ oxygen electrodes of solid oxide electrolysis cells

Yanxiang Zhang,[a, b] Kongfa Chen,[c] Changrong Xia,[a] San Ping Jiang,[c] Meng Ni[b, *]

[a] CAS Key Laboratory of Materials for Energy Conversion, Department of Materials Science and Engineering, University of Science and Technology of China, Hefei, 230026 Anhui, China

[b] Building Energy Research Group, Department of Building and Real Estate, The Hong Kong Polytechnic University, Hung Hom, Kowloon, Hong Kong, China

[c] Fuels and Energy Technology Institute and Department of Chemical Engineering, Curtin University, Perth, WA 6102, Australia

* Corresponding author, Tel: +852-2766-4152, Fax: +852-2764-5131, Email: meng.ni@polyu.edu.hk

Abstract

A theoretical model is developed to simulate the delamination kinetics of $La_{0.8}Sr_{0.2}MnO_3$ (LSM) electrode from YSZ electrolyte in solid oxide electrolysis cells (SOECs). The delamination is caused by the total stress including the internal oxygen pressure in LSM near the electrode/electrolyte interface, and the tensile stress by the oxygen migration from the

YSZ electrolyte to LSM lattice. Weibull theory is used to determine the survival probability of electrode/electrolyte interface under the total stress. The relaxation time corresponding to the time for oxygen diffusion from the interface to the microcracks in $La_{0.8}Sr_{0.2}MnO_3$ links the survival probability with polarization time, thus the survival interface area can be predicted with varying anodic polarization time. The model is validated with experimental data. The effects of applied anodic current and operating temperature are discussed. The present model provides a starting point to study more complex cases, such as composite oxygen electrodes.

Keywords: Solid oxide electrochemical cells; Delamination; Model; Degradation; Weibull theory

1. Introduction

Solid oxide electrolysis cells (SOEC) have received greater attention as efficient and environmentally friendly devices for hydrogen and syngas generation [1]. A typical SOEC cell consists of at least three functional layers: oxygen electrode, electrolyte, and fuel electrode. All of these components should provide good mechanical compatibility and chemical stability to function well in the respective environments – highly reducing for the fuel electrode and strongly oxidizing in the oxygen electrode at 800 ^{o}C – 900 ^{o}C, which puts rigorous requirements for materials. To date, Sr-doped $LaMnO_3$ (LSM) perovskite is the most widely used and studied oxygen electrode material, while the electrolyte and fuel electrode are typically made of yitria-stabilized zirconia (YSZ) and Ni/YSZ cermet, respectively. Performance degradation due to various failure processes is a major obstacle to practical

application of SOECs. Particularly, the delamination of LSM oxygen electrode at the electrode/electrolyte interface is the most common mode of failure [2]. For instance, Knibbe et al. [3] observed the pore formation in the grain boundaries of YSZ electrolyte near the interface of the electrolyte and the composite LSM-YSZ oxygen electrode polarized at high current densities. Laguna-Bercero et al. [4] studied the degradation of a tubular SOEC under high voltages, and observed the pore formation along the grain boundaries of YSZ electrolyte and the delamination of the composite LSM-YSZ electrode. Chen and Jiang [2] investigated the failure mechanism of $La_{0.8}Sr_{0.2}MnO_3$ oxygen electrodes under a constant anodic current passage and observed the complete delamination of $La_{0.8}Sr_{0.2}MnO_3$ electrode from YSZ electrolyte. Some other related studies can be also found in the references of these literatures [2-5].

In general, the delamination is considered to be caused by the build-up of high oxygen pressure in the YSZ electrolyte just near the electrolyte/oxygen electrode (LSM based) under an anodic polarization. Recently, Virkar [6] theoretically derived the oxygen pressure in the electrolyte near the electrolyte/oxygen electrode interface for simulating the degradation of SOEC cells. The model showed that the electronic conductivity of YSZ electrolyte, although small, should be taken into account for determining local oxygen chemical potential within the electrolyte. Rashkeev et al. [7] developed an atomic-scale model to reveal the mechanisms of LSM oxygen electrode delamination from YSZ electrolyte. Their calculation showed that migration of La, Sr, and Mn atoms from LSM electrode into YSZ electrolyte could cause a high oxygen pressure inside the void or pore, which contains a lot of defects and grain boundaries exhibiting electronic conductivity. However, due to the steady-state

nature of their model, it cannot predict the delamination kinetics. In addition, these models focus on the disintegration of YSZ electrolyte, and may be not sufficient to explain some other experimental observations. For example, when $La_{0.8}Sr_{0.2}MnO_3$ is used as the oxygen electrode, nanoparticles are formed within LSM grains at the LSM electrode/YSZ electrolyte interface prior to the delamination of LSM oxygen electrodes [2]. Detailed discussion and explanation of this observation is provided in section 2 – model.

In this work, a simple theoretical model is developed to capture the delamination kinetics of $La_{0.8}Sr_{0.2}MnO_3$ oxygen electrodes supported by YSZ electrolytes. The model is validated by comparing the modeling results with experimental data from [2] and additional experimental data. Experimental procedure for the additional experimental data can be found in Ref [2]. The effects of anodic current passage and operating temperature on the delamination kinetics will be discussed. The theoretical model is demonstrated to be a simple and easy to implement tool and can be integrated into 2D or 3D models to simulate the SOEC performance degradation at cell or stack level.

2. Model

According to Virkar's model [6], the oxygen pressure in YSZ electrolyte just near the LSM electrode/YSZ electrolyte interface can be determined as,

$$P_{O_2} = P_{O_2}^{ox} \exp\left[-\frac{4F}{RT}\left\{ \frac{E_A}{R_e} r_e^a - \frac{E_A - E_N}{R_i} r_i^a \right\} \right] \quad (1\text{-a})$$

where,

$P_{O_2}^{ox}$: oxygen pressure in the gas phase at the oxygen electrode, MPa;

E_A (E_N): applied (Nernst) voltage, V;

r_i^a (r_e^a): ionic (electronic) interface resistance at the LSM electrode/YSZ electrolyte interface, Ωcm^2;

R_i (R_e): ionic (electronic) resistance of the cell, Ωcm^2;

F, *R*, and *T* have the usual meaning.

It is known that the electronic conductivity of YSZ is extremely small, and thus R_e may be dominated by the YSZ electrolyte. Accordingly, $\frac{E_A}{R_e} r_e^a$ is assumed to be zero. It should be noted that the term $\frac{E_A - E_N}{R_i} r_i^a$ is the anodic overpotential at the LSM electrode/YSZ electrolyte interface. Eq. (1-a) can be approximatively rewritten as,

$$P_{O_2} = P_{O_2}^{ox} \exp\left[\frac{4F}{RT}\eta\right] \quad (1\text{-b})$$

Here, the sign of anodic overpotential, η (V) is positive. Eq. (1-b) has the same form with Nernst equation, and is also used to discuss the durability of SOEC cells by Knibbe et al [3, 8]. However, the governing factors, such as η and $P_{O_2}^{ox}$ should be treated carefully when considering the specific interface structure. Fig. 1a sketches a LSM oxygen electrode/YSZ electrolyte system operated in SOEC mode. It is observed that the LSM particles in contact with YSZ electrolyte disintegrate into nanoparticles in the range of 50 - 100 nm at the interface, leading to complete delamination of LSM electrode [2]. More importantly, the nanoparticles or microcracks originate at the inner interface region. In other words, at the initial stage of delamination, the three-phase boundary (TPB) region where LSM, YSZ and pore meet or the contact ring between LSM and YSZ (Fig. 1a) still connects the LSM electrode to the YSZ electrolyte tightly, while the nanoparticles have been formed within the TPB contact rings. This is attributed to the strong bonding between the edge of LSM grains

and YSZ rings formed by high temperature sintering [9]. Another possible reason may be the release of internal oxygen pressure near the TPB region. From Eq. (1-b) and the three-electrode configuration in Fig. 1a, the overpotential, η near the TPB region is smaller than that at the inner LSM/YSZ interface region due to the potential distribution in YSZ electrolyte. Thus the oxygen pressure built up in YSZ near the TPB region is smaller than that at the inner interface region. As the delamination is caused by the propagation of nanoparticles constrained within the TPB region, the overpotential should also be focused on the inner interface region. Thus the three-electrode arrangement is ideal for the overpotential measurement in this case. Fig. 1b shows the Tafel plots of anodic current – overpotential for a $La_{0.8}Sr_{0.2}MnO_3$ oxygen electrode supported by an YSZ electrolyte measured by three-electrode arrangement at 800 ^{o}C under various oxygen pressures. As is shown, the environmental oxygen pressure has little effect on the overpotential curves. The linear segments of experimental data extrapolate to a current density of 5×10^{-3} Acm^{-2}, which can be used to estimate of the exchange current density [10].

There exist different understandings about the physical meaning of $P_{O_2}^{ox}$. Virkar [6] considered $P_{O_2}^{ox}$ as the oxygen pressure in the gas phase at the oxygen electrode. That is, if the environmental oxygen pressure is decreased, the internal oxygen pressure, P_{O_2} will be decreased, which can slow down the delamination process. On the contrary, the atomic-scale model by Rashkeev et al. [7] suggested that increasing oxygen pressure by e.g., providing an additional oxygen flow through the oxygen electrode could slow down the migration of cations from LSM to YSZ electrolyte, and thus increase the lifetime of SOEC cells. To understand the effects of environmental oxygen pressure on the delamination kinetics,

purposely designed experiments have been conducted. Two batches of $La_{0.8}Sr_{0.2}MnO_3$ oxygen electrodes supported by YSZ electrolytes were polarized under a 500 $mAcm^{-2}$ anodic current passage at 800 ^oC in air and pure oxygen conditions, respectively. The electrode polarization resistances under an open-circuit condition were defined as charge-transfer resistances in ref. [11], R_p, Ωcm^2, and are measured as a function of polarization time. The results are shown in Fig. 1c. The absolute values of R_p in pure oxygen condition are smaller than that in atmospheric air. It is evident that an increase of environmental oxygen pressure can facilitate the charge-transfer process. However, it is important to note that both sets of data have similar kinetics with polarization time. The evolution kinetics behaves like the bathtub curve [12], and can be divided into three stages – initial activation stage, stable polarization stage, and degradation stage [2]. It was observed that the infancy microcracks have been formed in the initial activation stage, and the $La_{0.8}Sr_{0.2}MnO_3$ oxygen electrodes for these two cases completely delaminate from the YSZ electrolyte after polarization for 48 hours. This experimental observation indicates that the environmental oxygen pressure has insignificant effect on the delamination kinetics. Accordingly, the $P_{O_2}^{ox}$ in Eq. (1-b) should correspond to the equilibrium oxygen pressure in the bulk of LSM particles, $P_{O_2}^{eq}$, which is independent of environmental oxygen pressure during the lifetime of LSM oxygen electrode due to its low oxygen diffusion coefficient. Consider the raw LSM powder is exposed to the air during its synthesis and storage processes, it is reasonable to assume $P_{O_2}^{eq}$ as the oxygen pressure in air. Thus, Eq. (1-b) is rewritten as,

$$P_{O_2} = P_{O_2}^{eq} \exp\left[\frac{4F}{RT}\eta\right] \tag{1-c}$$

It should be emphasized that P_{O_2} in Eq. (1-c) represents the oxygen pressure built up in

YSZ electrolyte close to electrode/electrolyte interface, which is derived from the concept of local thermodynamic equilibrium [6]. Furthermore, the local equilibrium also suggests that the chemical potentials of oxygen in YSZ and LSM near the LSM/YSZ interface must be the same. Thus, the corresponding oxygen pressures must be the same. Therefore, P_{O_2} can also represent the oxygen pressure in LSM near LSM/YSZ interface. Interestingly, this treatment has been used to model the mixed ionic-electronic conducting electrodes, such as $La_{0.6}Sr_{0.4}Co_{0.2}Fe_{0.8}O_3$ (LSCF) [13]. The electrode overpotential, η directly relates with the oxygen pressures in LSCF at the electrode interface and the electrode bulk, with which the LSCF material could be in equilibrium due to the local oxygen ion concentration or the local oxygen nonstoichiometry. Mizusaki et al. [14] studied the oxygen nonstoichiometry, d of $La_{1-x}Sr_xMnO_{3+d}$ as a function of equilibrium oxygen pressure, P_{O_2}. It is found that, in oxygen-excess region ($d > 0$), the cation vacancies are predominantly located on the La site. The chemical formula of $La_{1-x}Sr_xMnO_{3+d}$ was revised as $[La_{1-x-a+ax/2}Sr_{x(2-a)/2}V_a][La_{a/2}Mn_{(2-a)/2}]O_3$, where V represents an A-site vacancy and a is the vacancy concentration or site fraction. A defect model was proposed to rationalize the a vs. P_{O_2} relationship [14],

$$a^6\left[1-3x\left(1-a/2\right)-9a+ax/2\right]^{-2/3}=P_{O_2}/P_{O_2}^{*} \quad (2)$$

where $P_{O_2}^{*}$ is the characteristic pressure relates with the vacancy equilibrium (MPa), and is a function of Sr-doped content, x and absolute temperature, T, $P_{O_2}^{*} = A\exp(-B/T)$. The values of A and B for $La_{0.8}Sr_{0.2}MnO_3$ are listed in Table 1. Fig. 1d shows the plot of Eq. (2) and the experimental data extracted from Ref. [14]. It is considered that the local tensile stress induced by oxygen migration from YSZ electrolyte to LSM lattice and the oxygen pressure in

LSM near the interface results in the microcrack and nanoparticle formation at the interface and the complete delamination of LSM electrode [2], the total stress can be estimated as $E\theta a + P_{O_2}$, where E is the Young's module (GPa), θ is the chemical expansion coefficient (dimensionless).

The Weibull theory has been successfully applied to study the structure failure of solid oxide fuel cells [15-18]. According to Weibull's theory, the complete expression for the survival probability ($P_{s,0}$) of a brittle material can be determined as [19-21],

$$P_{s,0} = \exp\left[-\int_V \left(\frac{\sigma}{\sigma_0}\right)^m \frac{dV}{V_R}\right] \tag{3-a}$$

where σ_0 is the characteristic strength (MPa) often taken to be the mean strength of the material [19], m is the Weibull module (dimensionless), measuring the variability of the strength of the material [19]. The reference volume (V_R) is linked to the characteristic strength. According to Weibull model, the survival probability of the reference volume (V_R) can be evaluated as [19].

$$P_{s,0}(V_R) = \exp\left[-\left(\frac{\sigma}{\sigma_0}\right)^m\right] \tag{3-b}$$

It means that at a tensile stress of σ_0, the survival probability is 1/e, that is, 37% [19]. Therefore, the choice of reference volume V_R could influence the value of characteristic strength σ_0 [20]. In the literature the reference volume for LSM electrode was reported to be about 1.21mm^3 [22,23]. In these studies, the whole porous LSM material is subjected to tensile stress and the Weibull parameters are obtained by fitting the experimental data with the Weibull model. However, in the present study, delamination only occurs at the interface between the LSM electrode and YSZ electrolyte [2]. Considering that the LSM layer is not

limited and its weight can be neglected, only the LSM/YSZ interfacial region is subjected to tensile stress while no stress exists inside the porous LSM layer. Therefore, the reference volume for the bulk LSM ($1.21mm^3$) is not applicable to the present study. It should correspond to the LSM/YSZ interfacial region (Figure 1a). Accordingly, a characteristic strength σ_0 for the interfacial region should be used. However, due to the limited data in the literature, a value of characteristic strength σ_0 from reference [26] is used. In general, the integral volume, *V* in Eq. 3-a corresponds to the studied domain or the region where structure failure may occur. Thus, according to Weibull model, for a given set of parameters, the survival probability should increase with decreasing V [19]. However, in the present study, only the interface between the LSM electrode and YSZ electrolyte is subjected to tensile stress, the survival probability is related to the current density and interfacial material properties, but independent of the LSM thickness. In the present study, the integration volume (V) is considered to be equivalent to the reference volume V_R. This assumption allows the Eq. 3-b to be used to calculate the survival probability at the interfacial region instead of Eq. 3-a. The validity of the simplification needs to be checked, but this point is out of the scope of the paper. Therefore Eq.3-b has been used in this study since it gives trends which are consistent with experimental findings. However, validation is needed when extending the present study to other configurations. As the stress at the interfacial region can be expressed as, $\sigma = E\theta a + P_{O_2}$, the LSM/YSZ interface survival probability can thus be calculated as,

$$P_{s,0} = \exp\left[-\left\{\frac{E\theta a + P_{O_2}}{\sigma_0}\right\}^m\right] \quad \text{(3-c)}$$

To date, the Weibull parameters for SOFC materials are rarely available in the

literature and they were obtained only from macroscopic porous samples, e.g. by ring-on-ring tests. There is still a lack of systematic study on the size dependence of Weibull parameters. Recently, our research group measured the Weibull parameters of micron scale fracture of YSZ particles and did not find strong size-dependence [24]. However, it should be mentioned that the interfacial stability is enhanced significantly when the particle size is at nano-scale (i.e. the infiltrated nanoparticles) [15]. Therefore, we employ the Weibull parameters combining with the Young's modulus of porous LSM as a starting point (Table 1). Thus the survival interface area (cm^2) can be,

$$S = S_0 P_{s,0} \tag{4-a}$$

where S_0 is the initial interface area between LSM and YSZ. It should be noted that Eq. (1-c) was derived based on the local equilibrium but global non-equilibrium concepts. According to the experimental observations, the electrode delamination is induced gradually by the formation of LSM nanoparticles layers with 50 – 100 nm thickness, which indicates a relaxation time, τ for the oxygen diffusion from the LSM/YSZ interface to the microcracks in LSM close to the interface. As thus, the survival interface area can be determined as,

$$S = S_0 P_{s,0}^{\,t/\tau} \tag{4-b}$$

According to the Fick's diffusion law [25], the relaxation time can be estimated roughly as, $\tau \sim l^2/D$, where l is the characteristic diffusion length, D is the oxygen diffusion coefficient. For example, the relaxation time at 800 ^oC will be 2.7 hours if we consider l = 100 nm and D = 1×10^{-14} cm^2/s [27]. It is found that 2 hours' relaxation at 800 ^oC agrees well with experiments.

The current density can be linked with overpotential using the Butler-Volmer equation,

$$i = i^* \frac{TPBL}{TPBL_0}\left\{\exp\left[\alpha\frac{4F\eta}{RT}\right] - \exp\left[-(1-\alpha)\frac{4F\eta}{RT}\right]\right\} \tag{5}$$

where i* is the exchange current density (Acm^{-2}) corresponding to the initial TPB length

density, $TPBL_0$ (cm.cm^{-2}), $TPBL$ is the TPB length after delamination (cm.cm^{-2}), α is the transfer coefficient (dimensionless). Due to the complex TPB configuration at the electrode/electrolyte interface, it is difficult to exactly determine $TPBL$. But it is rational to use the ratio of interface areas, S/S_0, to represent the ratio of TPB lengths, $TPBL/TPBL_0$, because the contact rings distribute uniformly at the electrode/electrolyte interface. It should be noted that such an approach does not take into account the slight increase in active TPB sites at the initial stage of delamination as result of the microcracks formation within the contact rings induced by the high partial pressure [2]. Compared with the decrease of TPB length in other delamination stages, this increase is negligible. Accordingly, under a constant applied current passage ($i = i_0$), we have,

$$i_0 = i^* \frac{S}{S_0}\left\{\exp\left[\alpha\frac{4F\eta}{RT}\right] - \exp\left[-(1-\alpha)\frac{4F\eta}{RT}\right]\right\} \tag{6}$$

Combining with Eq. (1-c), the oxygen pressure can be expressed as a function of current density. For the case $\alpha = 1$, it suggests a linear relationship,

$$P_{O_2} = P_{O_2}^{eq}\left[1 + (i_0 / i^*)(S_0 / S)\right] \tag{7}$$

For a common case such as $\alpha = 0.5$, it leads to a quadratic relation, $P_{O_2} = \frac{P_{O_2,pore}}{4}\left(\sqrt{(i_0/i^*)^2(S_0/S)^2 + 4} + \frac{i_0}{i^*}\frac{S_0}{S}\right)^2$, which usually suggests a very high oxygen pressure. For instance, consider $i_0 = 0.5$ Acm^{-2} at 800 ^{o}C under air condition ($i^* = 5\times10^{-3}$ Acm^{-2}, Table 1), the quadratic relation leads to a pressure of 210 MPa at the beginning of polarization ($S = S_0$), which is much higher than the characteristic strength of LSM, 52 MPa (Table 1). LSM electrode may delaminate from YSZ electrolyte immediately under this pressure. But experimental observations show the complete delamination occurs after

polarization for 48 hours under this condition. In fact, the transfer coefficient can vary with the anodic current. For current passage below 0.1 Acm^{-2} shown in Fig. 1b, the best fitting result is $\alpha = 0.24$. But when the applied anodic current is relative high, e.g., 0.1 ~ 1 Acm^{-2}, the Butler-Volmer equation suggests $\alpha = 1$. In this work, the anodic current passages are 0.5 Acm^{-2} and 1 Acm^{-2}. Based on the experimental measurements, the transfer coefficient of $\alpha = 1$ is used and this can be also a first-order correction of the reduced overpotential at the initial stage of polarization. According to Eq. (5), the oxygen pressure can be estimated as a function of polarization time,

$$P_{O_2} = P_{O_2}^{eq}\left\{1+\frac{i_0}{i^*}\exp\left[\left(\frac{E\theta a + P_{O_2}}{\sigma_0}\right)^m \frac{t}{\tau}\right]\right\} \quad (8)$$

Note the oxygen pressure (P_{O_2}) represents the pressure at the microcracks in LSM. Combining Eq. (2) with Eq. (8), the total stress induced by lattice shrinkage and the internal oxygen pressure can be determined as a function of polarization time. Further, the survival interface area or the fraction of survival interface can be estimated by using Eq. (4-b).

3. Results and discussion

The polarization resistances at open-circuit condition or charge transfer resistances (R_p, Ωcm^2) for $La_{0.8}Sr_{0.2}MnO_3$ electrode at various applied current passages and operating temperatures are measured as a function of polarization time to validate the model. As a starting point, R_p is assumed to be inversely proportional to the survival interface area,

$$R_p = R_{p,0}\exp\left[\left\{\frac{E\theta a + P_{O_2}}{\sigma_0}\right\}^m \frac{t}{\tau}\right] \quad (9)$$

where $R_{p,0}$ is the initial polarization resistance. Therefore, the electrode delamination

(decrease of *S*) kinetics is expressed by the increase of the charge transfer resistance. Therefore, one limitation of the model is that it cannot capture the initial activation (Fig. 1c), which relates to the improvement of oxygen oxidation reaction by the infancy microcracks [2]. However, it is capable of simulating the delamination kinetics in all other stages. The model input parameters, including the mechanical, chemical, and electrochemical parameters from Refs. [14, 26-29] and experimental determination are summarized in Table 1.

Fig. 2a shows the effects of anodic current passage. The scatter symbols are experimental data, and the solid lines are modeling results. As is shown, when the $La_{0.8}Sr_{0.2}MnO_3$ electrode is polarized under an anodic current of 1000 $mAcm^{-2}$ at 800 ^oC, it gradually delaminates from YSZ electrolyte, and the complete delamination occurs after 22 hours' polarization. When the applied current is decreased to 500 $mAcm^{-2}$, the delamination process is slowed down, and the complete delamination is observed after 48 hours' polarization. The calculation results agree nicely with the experimental data. When the anodic current is decreased to 200 $mAcm^{-2}$, the electrode lifetime is predicted as 128 hours. It is interesting to note that the electrode lifetime seems to be in inverse proportion to the anodic current density. In other words, the electrode lifetime can be improved to an acceptable degree by decreasing the applied current. As thus, the utilization of composite LSM-YSZ electrode may alleviate or even prevent the delamination, because the applied current is distributed in the electrode bulk, rather than at the electrode/electrolyte interface only. The magnitude of the microcrack and nanoparticles induced delamination kinetics at the composite electrode/YSZ electrolyte interface will be substantially smaller. Thus, the degradation mode of SOEC cells with composite LSM-YSZ electrode would need to take

into account the formation of micropores/holes in YSZ electrolyte pushed by the oxygen evolved near electrode/electrolyte interface [3, 4]. The present model is specific for the LSM oxygen electrode, and does not consider the holes formation in YSZ electrolyte, but it provides a basic understanding on the delamination kinetics as a starting point.

As known, the electrolysis reaction is endothermic [1], as such the increase of operating temperature increases the thermal energy demand and decreases electrical energy. Fig. 2b shows the effects of operating temperature on electrode resistance under an anodic current of 500 $mAcm^{-2}$. It is found that the electrode lifetime decreases drastically with increasing operating temperature. For example, when the operating temperature is increased from 800 ^{o}C to 900 ^{o}C, the electrode lifetime is decreased from 48 hours to 2 hours. According to Eq. (8), it may be caused by the combined effects of exchange current density, i^*, vacancy concentration, θ, and relaxation time, τ. Therein, i^* and θ have positive effects on improving the electrode lifetime. As shown in Table 1, when the temperature is increased from 800 ^{o}C to 900 ^{o}C, i^* is increased from 5×10^{-3} Acm^{-2} to 1.1×10^{-2} Acm^{-2}. In addition, the vacancy concentration is decreased when the temperature is increased (Fig. 1d), indicating a decrease of the internal stress. But the relaxation time may have a negative effect on electrode lifetime. As discussed above, τ relates with the oxygen diffusion coefficient of LSM as, $\tau \sim l^2/D$, and D increases exponentially with temperature (Table 1). Thus increasing temperature shortens the relaxation time, leads to a faster delamination process. In this work, τ is treated as a fitting parameter, but its value is dominated and is basically in inverse proportion to the oxygen diffusion coefficient (Table 1). Note that the results are for $La_{0.8}Sr_{0.2}MnO_3$ electrodes. For other electrode materials, these mechanical, chemical, and electrochemical parameters should

be identified accordingly to fit the model.

4. Conclusions

Based on the experimental observations, we developed a kinetics model for the delamination of $La_{0.8}Sr_{0.2}MnO_3$ electrodes supported by YSZ electrolytes. The model is validated by comparing with experimental data. Calculation results show that the electrode lifetime is in inverse proportion to the applied anodic current, and the increase of operating temperature can shorten the electrode lifetime. The model has been shown to provide some basic understanding on the degradation kinetics of SOEC cells and can serve as a starting point for application in more complex cases.

Acknowledgments

Zhang YX and Xia CR would thank the financial support from the Ministry of Science and Technology of China (2012CB215403), China. Zhang YX and Ni M thank the support from The Hong Kong Polytechnic University (Project No. A-PL20), Hong Kong. Chen KF and Jiang SP thank the support from National Natural Science Foundation of China (U1134001), China and Australia Research Council (LP110200281), Australia.

References

[1] Ni M, Leung MKH, Leung DYC, Technological development of hydrogen production by solid oxide electrolyzer cell (SOEC), International Journal of Hydrogen Energy 2008; 33: 2337-2354.

[2] Chen K, Jiang SP, Failure mechanism of (La,Sr)MnO_3 oxygen electrodes of solid oxide

electrolysis cells, International Journal of Hydrogen Energy 2011; 36: 10541-10549.

[3] Knibbe R, Traulsen ML, Hauch A, Ebbesen SD, Mogensen M, Solid Oxide Electrolysis Cells: Degradation at High Current Densities, Journal of the Electrochemical Society 2010; 157: B1209-B1217.

[4] Laguna-Bercero MA, Campana R, Larrea A, Kilner JA, Orera VM, Electrolyte degradation in anode supported microtubular yttria stabilized zirconia-based solid oxide steam electrolysis cells at high voltages of operation, Journal of Power Sources 2011; 196: 8942-8947.

[5] Sohal MS, O'Brien JE, Stoots CM, Sharma VI, Yildiz B, Virkar AV, Degradation issues in solid oxide cells during high temperature electrolysis, Journal of Fuel Cell Science and Technology 2012; 9: 011017-10.

[6] Virkar AV, Mechanism of oxygen electrode delamination in solid oxide electrolyzer cells, International Journal of Hydrogen Energy 2010; 35: 9527-9543.

[7] Rashkeev SN, Glazoff MV, Atomic-scale mechanisms of oxygen electrode delamination in solid oxide electrolyzer cells, International Journal of Hydrogen Energy 2011; 37: 1280-1291.

[8] Knibbe R, Hauch A, Hjelm J, Ebbesen SD, Mogensen M, Durability of Solid Oxide Cells, Green 2011; 1: 141-169.

[9] Jiang SP, Wang, W, Effect of polarization on the interface between (La,Sr)MnO_3 electrode and Y_2O_3-ZrO_2 electrolyte, Electrochem. Solid-State Lett. 2005; 8: A115-A118.

[10] Bard AJ, Faulkner LR, Kinetics of Electrode Reactions in *Electrochemical Methods: Fundamentals and Applications* (John Wiley & Sons, Inc., New York, Chichester, Weinheim,

Brisbane, Singapore, Toronto, 2001), pp. 100-105.

[11] Park SM, Yoo JS, Peer Reviewed: Electrochemical Impedance Spectroscopy for Better Electrochemical Measurements, Analytical Chemistry 2003; 75: 455A-461A.

[12] Klutke GA, Kiessler PC, Wortman MA, A critical look at the bathtub curve, IEEE Transactions on Reliability 2003; 52: 125-129.

[13] Ruger B, Weber A, Ivers-Tiffee E, 3D-Modelling and Performance Evaluation of Mixed Conducting (MIEC) Cathodes, ECS Transactions 2007; 7: 2065-2074.

[14] Mizusaki J, Mori N, Takai H, Yonemura Y, Minamiue H, Tagawa H, Dokiya M, Inaba H, Naraya K, Sasamoto T, Hashimoto T, Oxygen nonstoichiometry and defect equilibrium in the perovskite-type oxides $La_{1-x}Sr_xMnO_{3+d}$, Solid State Ionics 2000; 129: 163-177.

[15] Zhang Y, Xia CR, A durability model for solid oxide fuel cell electrodes in thermal cycle processes, Journal of Power Sources 2011; 195: 6611-6618.

[16] Anandakumar G, Li N, Verma A, Singh P, Kim JH, Thermal stress and probability of failure analyses of functionally graded solid oxide fuel cells, Journal of Power Sources 2011; 195: 6659-6670.

[17] Cui D, Cheng M, Thermal stress modeling of anode supported micro-tubular solid oxide fuel cell, Journal of Power Sources 2009; 192: 400-407.

[18] Singhal SC, Kendall K, Cell, Stack and System Modelling in *High Temperature Solid Oxide Fuel cells: Fundamentals, Design and Applications* (Elsevier Ltd., Oxford, New York, Tokyo, 2003), p. 316.

[19] Meyers M, Chawla K, Mechanical Behaviors of Materials, Second Edition, Cambridge University Press, 2009, pp. 449-460.

[20] Danzer R, Lube T, Supancic P, Damani R, Fracture of ceramics, Advanced Engineering Materials 2008; 10, 275-298.

[21] Weibull W, A statistical distribution function of wide applicability, Journal of Applied Mechanics 1951; 18: 293-297.

[22] Atkinson A, Selcuk A, Proceedings of the 5th International Symposium on SOFC (SOFC V), Electrochemical Society, vols. 97-81 (1997), pp. 671-680.

[23] Atkinson A, Selcuk A, Mechanical behavior of ceramic oxygen ion-conducting membranes, Solid State Ionics 2000; 134, 59-66.

[24] Wang Y, Zhang Y, Xia C, A novel method to determine the particle-particle fracture of yttria stabilized zirconia, Journal of Power Sources; doi: 10.1016/j.jpowsour.2012.03.063.

[25] Balluffi RW, Allen SM, Carter WC, Solutions to the Diffusion Equation in *Kinetics of Materials* (John Wiley & Sons, Inc., Hoboken, New Jersey, 2005), pp. 113-114.

[26] Nakajo A, Stiller C, Gunnar H, Bolland O, Modeling of thermal stresses and probability of survival of tubular SOFC, Journal of Power Sources 2006; 158: 287-294.

[27] Berenov AV, MacManus-Driscoll JL, Kilner JA, Oxygen tracer diffusion in undoped lanthanum manganites, Solid State Ionics 1999; 122: 41-49.

[28] Bishop S, Duncan K, Wachsman E, Thermo-Chemical Expansion of SOFC Materials, ECS Transactions 2006; 1: 13-21.

[29] Chen X, Zhang L, Liu E, Jiang SP, A fundamental study of chromium deposition and poisoning at $(La_{0.8}Sr_{0.2})_{0.95}(Mn_{1-x}Co_x)O_{3\pm\delta}$ ($0.0 \leq x \leq 1.0$) cathodes of solid oxide fuel cells, International Journal of Hydrogen Energy 2011; 36: 805-821.

List of Figures

List of Table

Figure 1a

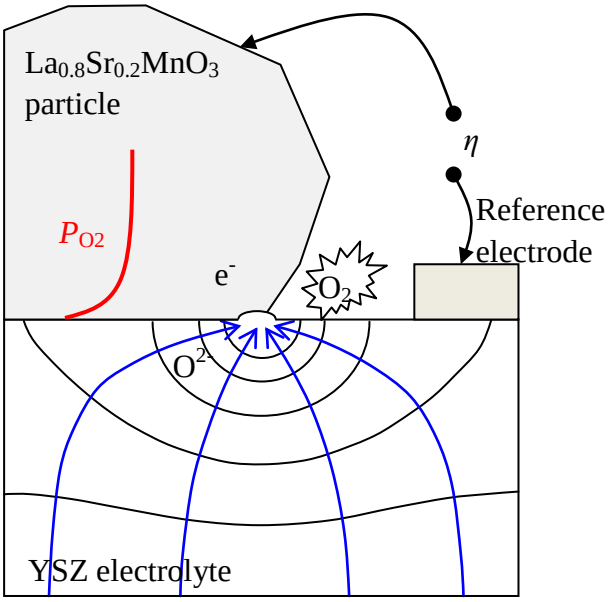

Figure 1b

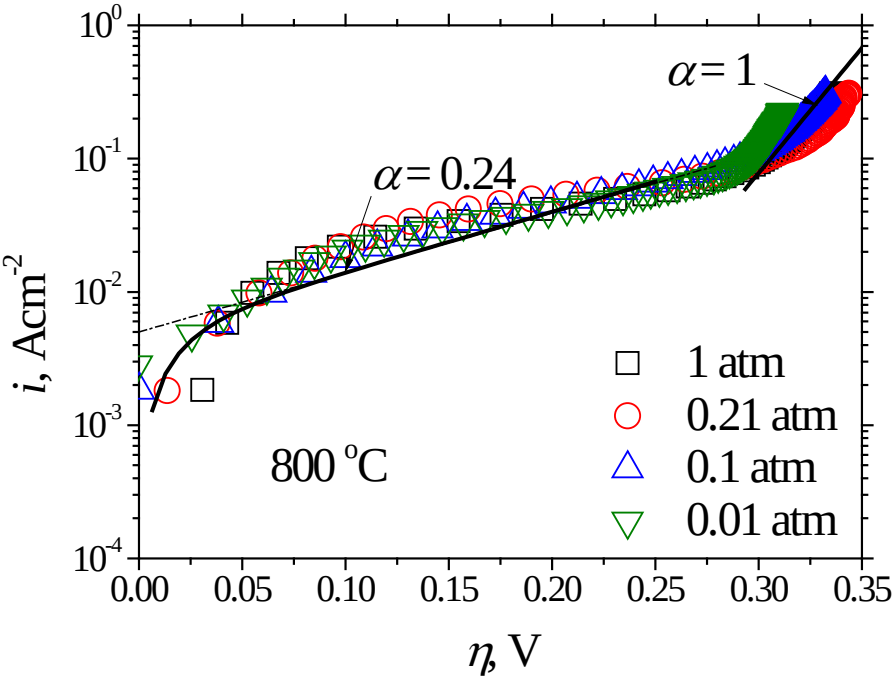

Figure 1c

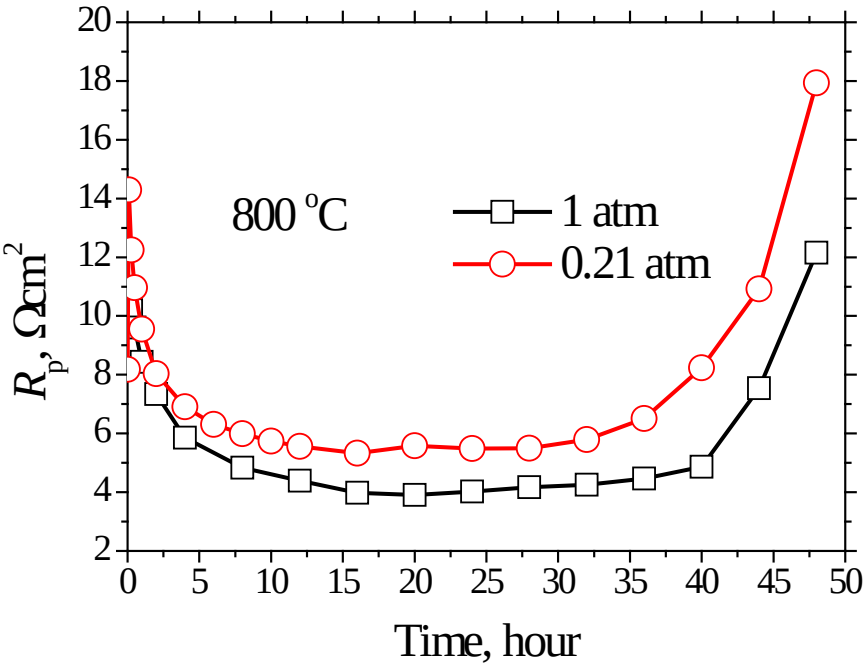

Figure 1d

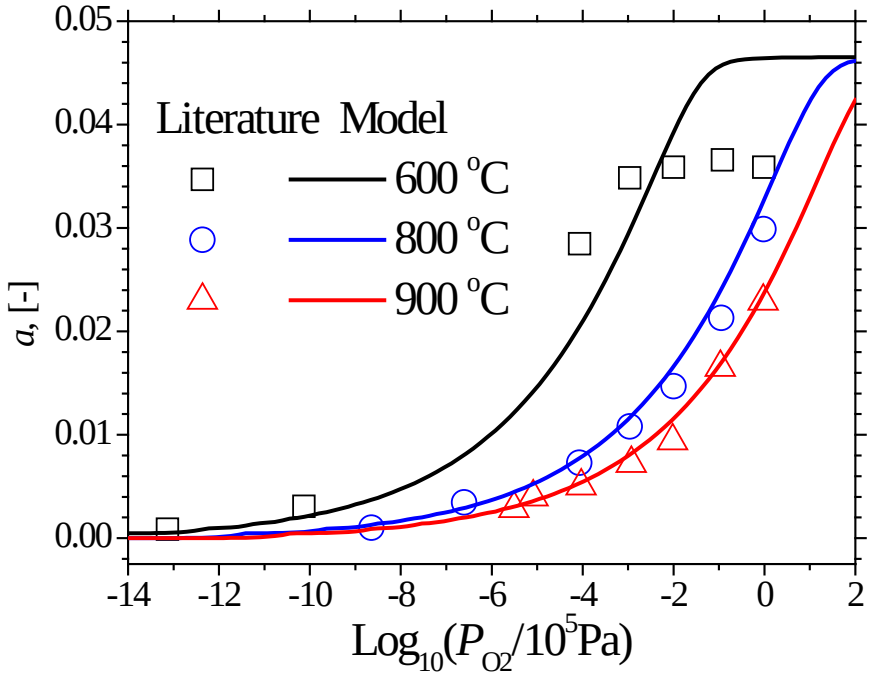

Figure 2a

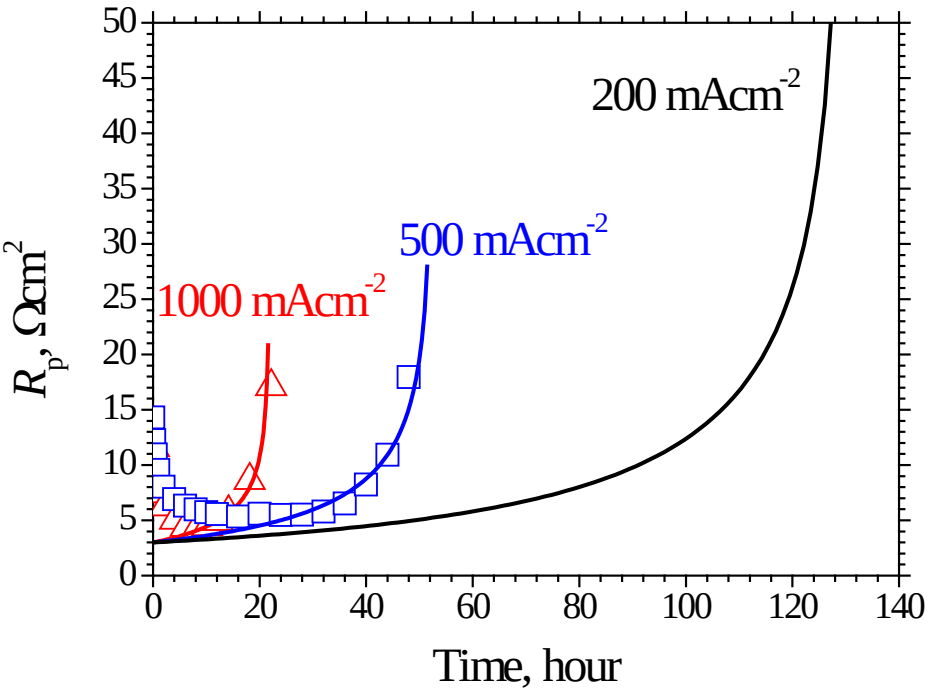

Figure 2b

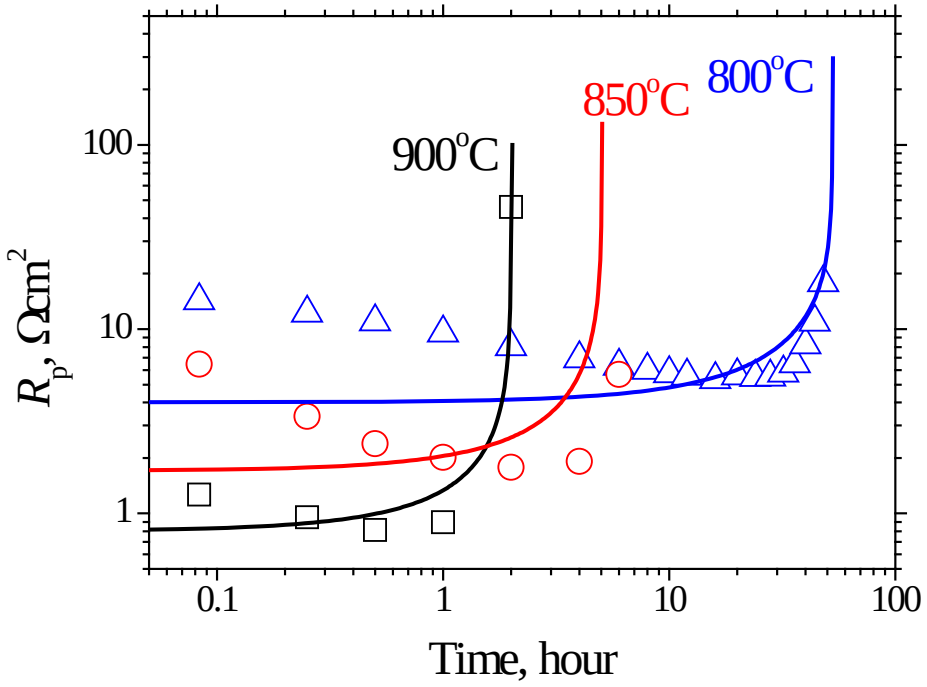

Table 1. Mechanical, chemical and electrochemical parameters for $La_{0.8}Sr_{0.2}MnO_3$ electrodes [14, 26-29].

E [26], GPa	θ [28,29],[a] [-]	σ_0 [26], MPa	m [26], [-]	A [14],[b] MPa	B [14],[b] K	T, K	$R_{p,0}$,[c] Ωcm^2	i*,[d] Acm^{-2}	D [27], cm^2s^{-1}	τ,[c] s
						1073	4.0	5×10^{-3}	1×10^{-14}	7200
35	1.94×10^{-2}	52	7	7.24×10^{18}	2.86×10^{4}	1123	1.7	9×10^{-3}	6×10^{-14}	225
						1173	0.8	1.1×10^{-2}	3×10^{-13}	33

[a] The chemical expansion coefficient for LSM is not available in literature yet, such the proposed data, 3.2×10^{-3} nm^3 for Gadolinium doped Ceria [28] is used. Considering the LSM lattice volume is about 0.1653 nm^3 [29], θ is estimated as 3.2×10^{-3} $nm^3/0.1653$ nm^3 = 1.94×10^{-2}.

[b] Recalculated results according to the experimental data and the defect model in Ref. [14].

[c] Fitting parameter.

[d] Experimentally determined.